

Magnetic properties of neptunium Laves phases: NpAl_2 , NpOs_2 , NpIr_2 , and NpRu_2 [†]

A. T. Aldred, B. D. Dunlap, D. J. Lam, and I. Nowik

Argonne National Laboratory, Argonne, Illinois 60439

(Received 20 March 1974)

The magnetic properties of a series of neptunium cubic C-15-type Laves phases (NpX_2 , where $X = \text{Al, Os, Ir, or Ru}$) have been studied between 1.5 and 300 °K by means of magnetization and nuclear γ -ray resonance measurements. The properties show a systematic variation with neptunium-neptunium distance d_{Np} . Thus, NpAl_2 ($d_{\text{Np}} = 3.37 \text{ \AA}$) is ferromagnetic with a transition temperature $T_c = 56 \text{ °K}$ and an ordered moment of $1.5 \mu_B/\text{mole}$; NpOs_2 ($d_{\text{Np}} = 3.26 \text{ \AA}$) is ferromagnetic with $T_c = 7.5 \text{ °K}$ and an ordered moment of $0.4 \mu_B/\text{mole}$; NpIr_2 ($d_{\text{Np}} = 3.25 \text{ \AA}$) is antiferromagnetic with $T_c = 7.5 \text{ °K}$ and an ordered moment of $0.6 \mu_B/\text{mole}$; and NpRu_2 ($d_{\text{Np}} = 3.23 \text{ \AA}$) does not order magnetically down to 1.5 °K. This trend is interpreted in terms of an increase in the delocalization of the neptunium magnetic moment and the magnetic $5f$ electrons, as d_{Np} decreases.

I. INTRODUCTION

Although the early actinide elements (uranium, neptunium, and plutonium) are nonmagnetic, a wide variety of their intermetallic compounds undergo long-range magnetic order.¹ The absence of long-range magnetic order in uranium, neptunium, and plutonium has been attributed to the degree of overlap of the $5f$ -electron wave functions on neighboring atoms (the $5f$ -electron wave functions are more spatially extended than the corresponding $4f$ -electron wave functions), which produces a $5f$ bandwidth too broad to support an ordered magnetic moment.² This bandwidth will also be effectively increased by hybridization of the $5f$ -electron states with the $6d$ - $7s$ - $7p$ conduction bands.³ In many actinide intermetallic compounds, the actinide-actinide distance is substantially greater than in the pure elements, and the overlap of the $5f$ wave functions is presumably much smaller; the $5f$ electrons are then essentially localized, the bandwidth is quite narrow, and magnetic ordering may occur. On the basis of such a simple argument, and an analysis of the literature, Hill⁴ showed that critical actinide-actinide spacings do exist in intermetallic compounds beyond which long-range magnetic ordering occurs.

If we focus on compounds of a single crystal-structure type in the region where the actinide-actinide distance is close to the critical value, then we might expect to see a systematic variation of magnetic properties with lattice parameter. As the actinide-actinide separation decreases toward the critical value, a change from localized to itinerant-electron magnetism should occur as the $5f$ electrons overlap and the $5f$ bandwidth increases. We have studied the magnetic properties of a series of NpX_2 compounds (where $X = \text{Al, Os, Ir, or Ru}$) with the C-15-type Laves-phase structure by means of magnetization and nuclear γ -ray resonance (NGR) measurements, and these properties

do vary in a systematic manner. The results support the concept of a change from localized to itinerant-electron behavior as the Np-Np distance decreases below a critical value.

II. EXPERIMENTAL

The compounds were prepared by arc melting the requisite amounts of the constituent metals in an argon-helium atmosphere. Chemical analysis of the electrorefined neptunium metal obtained from the Los Alamos Scientific Laboratory (used in this investigation) gave the following impurities (in weight ppm): Li < 1; Be < 1; Na < 10; Mg < 10; Al < 5; K < 5; Ca < 5; Ti < 1; V < 1; Cr < 1; Mn 3; Fe 5; Co < 1; Ni 6; Cu < 1; Zn 10; Rb < 1; Sr < 1; Y < 1; Zr < 1; Mo < 1; Cd < 1; Sn < 1; Cs < 5; Ba < 1; La < 1; Hf < 1; Re < 1; Pb 3; Th 5; U < 50; and Pu 526. The remaining materials used for compound preparation were zone-refined aluminum (99.9999% pure) high-purity iridium (99.95% pure), osmium (99.95% pure) and ruthenium (99.99% pure). The samples, weighing ~2 g, were arc melted three times, homogenized at temperatures between 800 and 1000 °C for several hours, and furnace cooled. X-ray powder patterns indicated that each sample was single phase with the C-15-type cubic Laves-phase crystal structure. Resistivity specimens were spark cut from the heat-treated buttons, and most of the remainder was powdered. Approximately 100 mg of each alloy was sealed in an aluminum capsule for magnetization measurements, and an additional 300–700 mg was sealed in a separate aluminum capsule for the NGR experiments.

Details of the equipment and techniques for the NGR measurements have been given previously⁵; hyperfine interaction constants and isomer shifts were obtained from 1.5 to 10 °K by means of the 59.6-keV resonance in ²³⁷Np. The magnetization results were obtained from 4 to 300 °K in fields between ~0.5 and ~13.5 kOe by a force method.

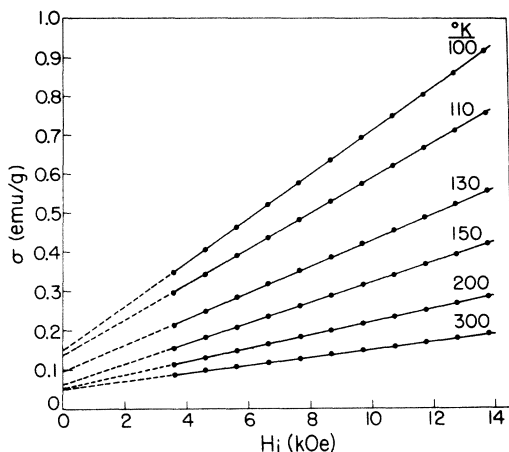


FIG. 1. Typical magnetization vs field plots for NpAl_2 between 100 and 300 °K.

The basic experimental arrangement has also been described previously,⁶ but, in an effort to automate the system, the techniques for data acquisition, reduction, and analysis have been changed and will be described here.

The force on the sample is measured by a Cahn model RH electrobalance; the temperature is monitored by a AuFe/Cu thermocouple, the junction of which is embedded in a copper-specimen support block in contact with the aluminum capsule containing the sample. This entire assembly is suspended from the balance arm by a 2-mm-diam thin-wall quartz tube. The AuFe/Cu thermocouple has the following advantages: (a) only a small contribution is made to the addenda correction, (b) sensitivity is essentially independent of temperature, and (c) almost no correction is required for magnetic-field effects. The thermocouple, which has an electronically controlled 0 °C reference junction, was calibrated at $\sim 2^\circ$ increments against a AuFe/Chromel thermocouple embedded in a dummy aluminum sample capsule. The voltage versus temperature relationship for the AuFe/Chromel thermocouple was taken from the NBS table,⁷ and a power-series fit of voltage versus temperature for the AuFe/Cu thermocouple was obtained. It is estimated that the accuracy of the temperature is $\pm 1^\circ \text{K}$, although the relative precision should be close to $\pm 0.2^\circ \text{K}$.

In operation, the voltage outputs from the balance and thermocouple are monitored sequentially, with the Varian electromagnet off, and recorded on paper tape. The magnet is switched on at the lowest setting (nominally 0.5 kOe) and, after a 30-sec delay to allow the field and balance reading to stabilize, the monitoring and recording process is repeated. The field is then increased at 1-kOe intervals up to 13.5 kOe, and readings are taken at each field. The field is then switched off, and,

after a 90-sec interval to allow the field to decay, the voltages are again recorded. This entire operation is controlled automatically, and after one sequence of readings is taken, the procedure is continuously repeated.

The experiment starts with the cryostat and sample at 4 °K. After one run at this temperature, the sample temperature is slowly increased ($\sim 0.5^\circ \text{K}/\text{min}$) by applying a voltage to a manganin heater on the tail section of the cryostat; this voltage is programmed to increase as a function of time. Data are accumulated continuously until a temperature of $\sim 300^\circ \text{K}$ is reached; this takes ~ 17 h and, after initial computer analysis, an array of $\sim 100 \times 14$ data points is obtained. Each point is a value of the specific magnetization σ (emu/g) at one of 14 applied fields H (Oe) and at a given temperature T (°K).

To evaluate the magnetization as a function of field at any particular constant temperature, we submit the data at each field to a cubic spline program, which determines an arbitrary interpolating function to give the magnetization for that field at any temperature between the maximum and minimum measured values. These functions are then stored within the computer and can be evaluated, when required, at any interpolated temperature.

The magnetic-field gradients at each applied field were calibrated internally with a high-purity single-crystal nickel sample [$\sigma(4.2^\circ \text{K}) = 58.57$ emu/g].⁸ The magnetic field was determined by a rotating coil gaussmeter ($\pm 0.1\%$) that had been calibrated against an NMR proton-probe gaussmeter in a different constant-field electromagnet.

III. RESULTS

A. NpAl_2

Some typical plots of magnetization versus internal field H_i in the temperature range (100–300) °K are shown in Fig. 1. (The internal field was obtained by subtracting an appropriate demagnetizing field based on the geometry and density of the sample from the applied field; over the temperature range of the data in Fig. 1 this correction is $< 0.1\%$ of H_i , whereas at lower temperatures the maximum correction is $\sim 3\%$ of H_i .) The linear field dependence of the magnetization is evident; the data at lower fields, not shown in Fig. 1, fall systematically below extrapolations of the linear field dependence, and this fact as well as the non-zero extrapolated values of σ at $H_i = 0$ suggest the presence of an easily saturated ferromagnetic component of the total magnetization. The susceptibility χ (emu/g Oe) was thus determined by least-squares fitting to an equation of the form

$$\sigma = \sigma_0 + \chi H_i, \quad (1)$$

where σ_0 represents the ferromagnetic component.

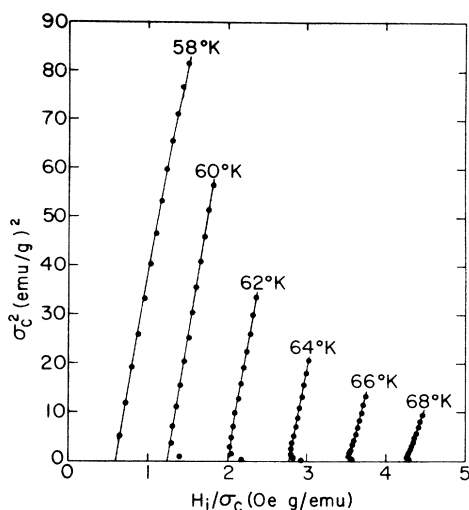


FIG. 2. Arrott plots for NpAl_2 at the temperatures indicated.

In view of the purity of the starting materials (Sec. II), it is difficult to ascribe the nonzero value of σ_0 to an impurity effect. The only known neptunium compound ferromagnetic at room temperature is NpFe_2 ,⁹ and 0.2% of NpFe_2 would be required in the sample to give the observed value of σ_0 . Every precaution was taken in cleaning the aluminum sample capsule prior to insertion in the apparatus. The only other possibility of sample contamination would occur during the capsule welding operation. Such contamination was unlikely because the operation was performed in a clean glovebox in an inert atmosphere. Also, the temperature dependence of σ_0 , to be shown later, suggests that the impurity is homogeneously distributed within the sample. NpAl_2 is the most stable phase (has the highest melting point) in the Np-Al phase diagram; it is a line compound and the adjacent phases are pure neptunium, which is not magnetically ordered, and NpAl_3 , which becomes ferromagnetic only at 62°K.¹⁰ The other potential source of a ferromagnetic component would arise from a lack of complete chemical ordering, which could produce neptunium-rich clusters that may order magnetically. However, the lack of any range of stoichiometry of the compound, the x-ray results, and the well-defined NGR spectra indicate that NpAl_2 is highly ordered.

It should be noted here that the presence of a σ_0 term is a rather general occurrence in neptunium compounds, including all compounds studied in the present work. The random nature of the magnitude of the term and its temperature dependence would indicate that σ_0 is not related to an experimental problem in the magnetization measurements.

Below 90°K, the magnetization versus field plots become curved, characteristic of the approach to a ferromagnetic transition. The data were sub-

jected to the usual Arrott plots¹¹ (H/σ vs σ^2), but the presence of a σ_0 component gave these plots a strongly curved low-field tail. To obviate this problem, data evaluated at 1°K intervals were fitted by an iterative least-squares procedure to the equation

$$H_i/(\sigma - \sigma_0) = A(\sigma - \sigma_0)^2 + B, \quad (2)$$

with σ_0 , A , and B ($\equiv \chi_0^{-1}$) treated as disposable parameters. Such a fit obviously presupposes a linear H/σ vs σ^2 relationship, whereas a more complicated expression may be appropriate. In fact, allowing σ_0 to vary produces reasonable linear plots as may be seen in Fig. 2, which shows H/σ_c vs σ_c^2 ($\sigma_c = \sigma - \sigma_0$) for several temperatures just above the Curie temperature T_c . (Because of experimental uncertainties, the higher field points are weighted more heavily in the least-squares analysis). For temperatures of 57°K and below, the fits did not converge, and this suggests that Eq. (2) is not appropriate in the temperature range close to and below T_c . On the basis of an extrapolation of the χ_0^{-1} values between 65 and 58°K, we estimate that $T_c = (56.5 \pm 1)^\circ\text{K}$. The fits yield $\sigma_0(68^\circ\text{K}) = 0.24$ emu/g and $\sigma_0(58^\circ\text{K}) = 1.32$ emu/g, compared with the value of $\sigma_0(300^\circ\text{K}) = 0.05$ emu/g. The rapid increase in σ_0 as the temperature approaches T_c presumably reflects the increase in response of the matrix to the ferromagnetic "impurity" as the matrix susceptibility increases.

The reciprocal molar susceptibility shows a smooth, slightly curved temperature dependence between 300 and 60°K (Fig. 3). A small anomaly occurs between ~170 and ~130°K that seems to be associated with the rapid increase in σ_0 in this

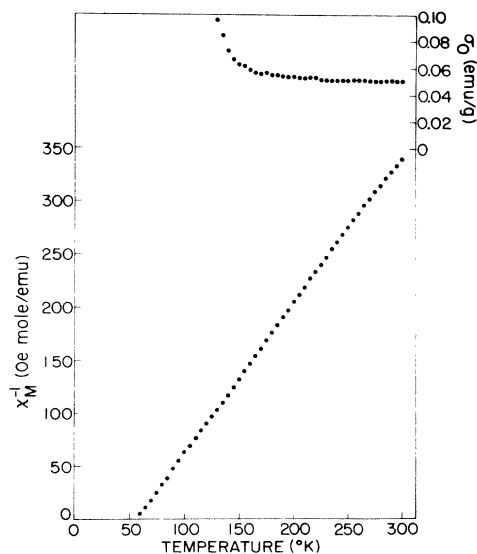


FIG. 3. Temperature dependence of the reciprocal molar susceptibility and σ_0 (see text) for NpAl_2 .

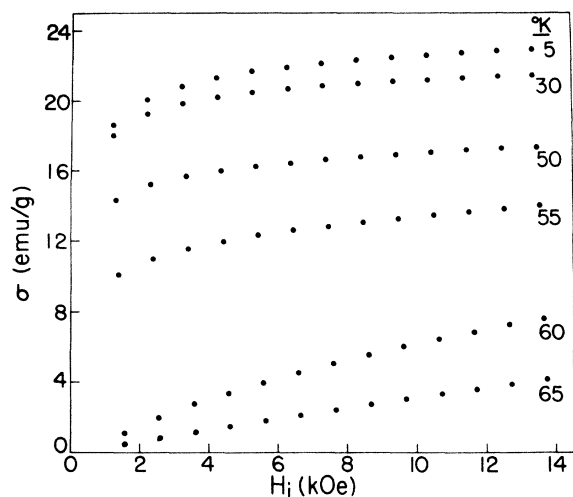


FIG. 4. Typical magnetization vs field curves for NpAl_2 between 5 and 65 °K.

temperature range (upper portion of Fig. 3). The scale for σ_0 was chosen, for reference purposes, to be the same for all compounds in this study, and the low-temperature values for NpAl_2 are too large to be plotted in Fig. 3.

The low-temperature magnetization data for NpAl_2 are plotted in Fig. 4. The field dependence at 5 °K is greater than at higher temperatures, and this is consistent with the presence of a large magnetocrystalline anisotropy that increases with a decrease in temperature; this behavior is typical of actinide ferromagnets.¹² Although the anisotropy constant (as well as the saturation magnetization) in a polycrystalline ferromagnet can, in principle, be determined from the H^{-2} dependence of the magnetization,¹³ such a procedure gives poor fits to the present data. The inclusion of a linear H (susceptibility) term improves the fit slightly, but the errors are still substantially greater than the experimental errors. The magnetization, in fact, appears to be saturating much more slowly than the conventional H^{-2} dependence, and this is, again, characteristic of actinide ferromagnets. Thus, we cannot determine a reliable saturation moment μ_{sat} for this compound from the present magnetization results. The magnetization at the maximum field (~ 13.5 kOe) at the lowest temperature corresponds to a moment of $1.19\mu_B/\text{mole}$.

We can obtain a reasonable estimate of the neptunium moment from the hyperfine field as determined by the NGR measurements. The NGR spectrum for NpAl_2 at 4.2 °K (Fig. 5) yields a neptunium hyperfine field of 2900 kOe. A constant relationship between the neptunium hyperfine field H_{hf} (in kOe) and the magnetic moment μ_{Np} (in Bohr magnetons), as determined by neutron-diffraction experiments, has been established in the neptunium mononitrides¹⁴

$$\mu_{\text{Np}} = (5.2 \times 10^{-4}) H_{\text{hf}}. \quad (3)$$

With this expression, an error of roughly $\pm 0.15\mu_B$ occurs in values of μ_{Np} derived from a given hyperfine field. The same constant is also found to apply to cubic NpPd_3 ,¹⁵ where the measured hyperfine field gives a moment of $(1.9 \pm 0.15)\mu_B$ in comparison with the neutron value $(2.0 \pm 0.1)\mu_B$. More importantly in the Laves-phase compounds NpNi_2 and NpFe_2 , the measured hyperfine fields¹⁶ give moments of $(1.4 \pm 0.15)\mu_B$ and $(0.9 \pm 0.15)\mu_B$, respectively, in comparison with neutron values¹⁷ of $(1.2 \pm 0.15)\mu_B$ and $(1.05 \pm 0.10)\mu_B$. Thus, in the subsequent discussion, we presume that Eq. (3) holds for the present compounds. The neptunium hyperfine field in NpAl_2 yields a moment of $1.5 \pm 0.15\mu_B/\text{Np}$, a value consistent with the slow approach to saturation of the magnetization data.

B. NpOs_2

The magnetization versus field curves for NpOs_2 in the range (30–300) °K are qualitatively similar to those of NpAl_2 shown in Fig. 1, i. e., the data between 3.5 and 13.5 kOe fit good straight lines that extrapolate to values of σ_0 which are nonzero but are at least a factor of 5 smaller than for NpAl_2 . Below 30 °K, the σ vs H plots become non-linear, and the data were treated in terms of Eq. (2), as in the case of NpAl_2 . In this manner, good straight-line plots of H/σ_c vs σ_c^2 were obtained down to 14 °K, with a value of σ_0 that increased only slowly with a decrease in temperature and was much smaller in magnitude (~ 0.03 emu/g) than the σ_0 value obtained for NpAl_2 . Below 14 °K, the data did not give a good fit to Eq. (2), and the values of σ_0 did not vary systematically with temperature. Accordingly, the weak temperature dependence of σ_0 above 14 °K was extrapolated down to 4 °K, and values of $\sigma_c = \sigma - \sigma_0$ were calculated and then plotted

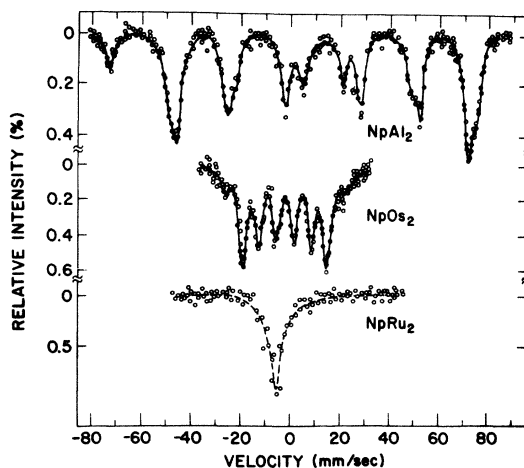


FIG. 5. NGR spectra for NpAl_2 , NpOs_2 , and NpRu_2 at 4.2 °K.

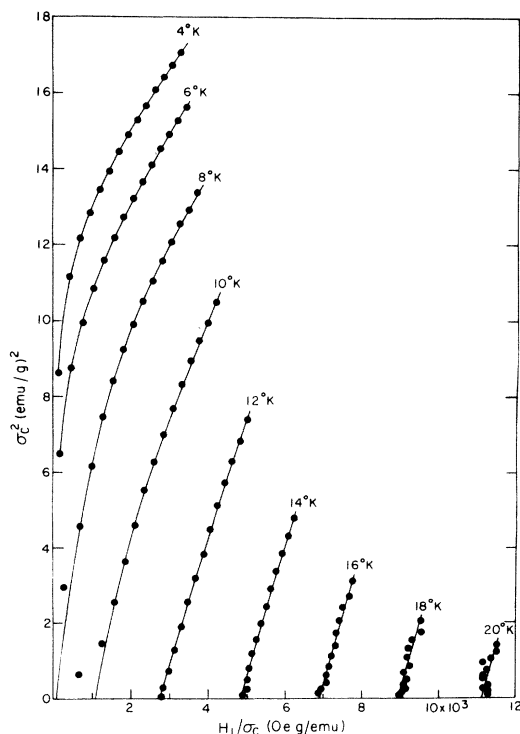


FIG. 6. Arrott plots for NpOs_2 at the temperatures indicated.

in the normal Arrott manner. Some of these data as well as data above 14°K that appear to be linear in H/σ_c vs σ_c^2 are shown in Fig. 6. The increasing curvature evident in the low-temperature data (Fig. 6) makes the extrapolation to determine χ_0^{-1} somewhat difficult. A detailed plot of χ_0^{-1} vs T below 30°K shows a linear region down to 12°K , which extrapolates to zero at 9°K . However, based on extrapolations of the data shown in Fig. 6, the χ_0^{-1} vs T plot below 12°K curves away from the temperature axis and yields a Curie temperature of $7.5 \pm 0.5^\circ\text{K}$. The value compares with $T_c = 7.4 \pm 0.5^\circ\text{K}$ determined by resistivity measurements¹⁸ and $T_c = 8.0 \pm 0.5^\circ\text{K}$ indicated by the Mössbauer data to be presented later. The Curie temperature for NpOs_2 appears to be much less well defined by the magnetization results (Fig. 6) than in the case of NpAl_2 (Fig. 2).

A plot of reciprocal molar susceptibility versus temperature for NpOs_2 is shown in Fig. 7. The data vary smoothly over most of the temperature range, although there may be an anomaly between ~ 70 and $\sim 30^\circ\text{K}$ similar to that seen at somewhat higher temperatures in NpAl_2 . However, in the case of NpOs_2 the anomaly is not associated with any rapid increase in σ_0 with a decrease in temperature, and is, apparently, an inherent feature of the material. The plot of σ_0 versus temperature is shown in the upper portion of Fig. 7. The term is much smaller than in NpAl_2 , and, although an

upturn is evident at low temperature as T_c is approached, the relative increase is again much smaller in magnitude than in NpAl_2 .

Some typical low-temperature magnetization data for NpOs_2 are plotted in Fig. 8. The lowest temperature corresponds only to $\sim 0.5T_c$, therefore, additional measurements were made in another apparatus at 1.8°K , and the field dependence follows the 4°K isotherm in Fig. 8 quite closely, although at a higher level. The field dependence of σ in NpOs_2 is similar to that in NpAl_2 . A careful examination of the data shows that the relative curvature is somewhat less in NpOs_2 , although the change in magnetization between 3.5 and 13.5 kOe at the lowest temperature is $\sim 15\%$ in NpOs_2 compared with only $\sim 10\%$ in NpAl_2 . If we take the ratio of $\mu_{\text{sat}}/\mu_{13.5}$ ($= 1.34$) for NpAl_2 and scale it to NpOs_2 based on the relative field dependence from 3.5 to 13.5 kOe, the moment at 13.5 kOe and 1.8°K for NpOs_2 ($= 0.46\mu_B/\text{mole}$) yields a saturation moment of $\sim 0.7\mu_B/\text{mole}$.

The NGR spectrum of NpOs_2 at 4.2°K is shown in Fig. 5. Measurements have also been made between 1.7 and 10°K ; extrapolation of the hyperfine field values determined from these spectra to absolute zero yields $H_{\text{hf}} = 815$ kOe, which converts, via Eq. (3), to a neptunium moment ($0.4\mu_B$) somewhat lower than that based on an approximate extrapolation of the magnetization data. The temperature dependence of the hyperfine field (Fig. 9) fits a $J = \frac{1}{2}$ Brillouin function, and a transition temperature of $8.0 \pm 0.5^\circ\text{K}$ is obtained from an analysis of the linewidth as a function of temperature. The hyperfine fields of other neptunium Laves phases have been found to follow a $J = \frac{1}{2}$ Brillouin function.¹⁹

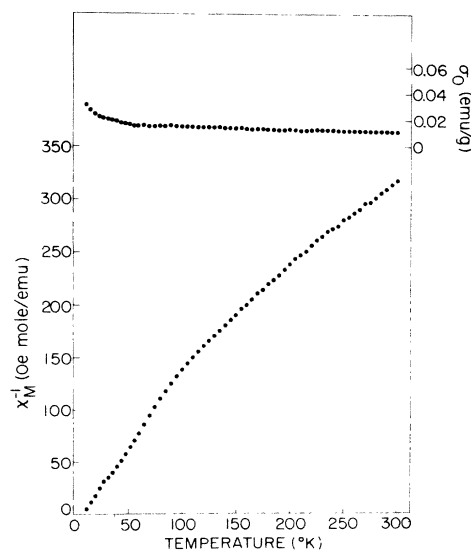


FIG. 7. Temperature dependence of the reciprocal molar susceptibility and σ_0 (see text) for NpOs_2 .

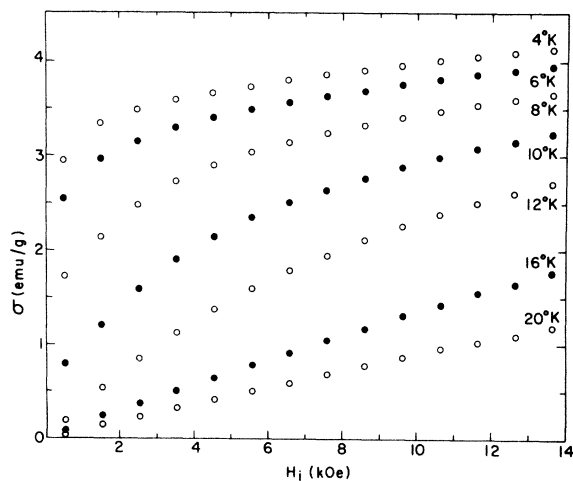


FIG. 8. Typical magnetization vs field curves for NpOs_2 between 4 and 20°K.

C. NpIr_2

The magnetization curves of NpIr_2 are linear from 1.5 to 13.5 kOe over the entire temperature range. The value of σ_0 is zero (within experimental error) from 300 to 250°K and increases slowly to reach a maximum value of 0.013 emu/g at the lowest temperatures. The small value of σ_0 is consistent with the greater range of linearity of the magnetization data (down to 1.5 kOe).

The reciprocal molar susceptibility is plotted as a function of temperature in Fig. 10, which also shows the small magnitude and weak temperature dependence of σ_0 . The two striking features of the susceptibility plot are the susceptibility maximum at 7.5°K, and the discontinuity near 220°K. The susceptibility maximum (see inset of Fig. 10) is characteristic of an antiferromagnetic transition; additional magnetization data were obtained down

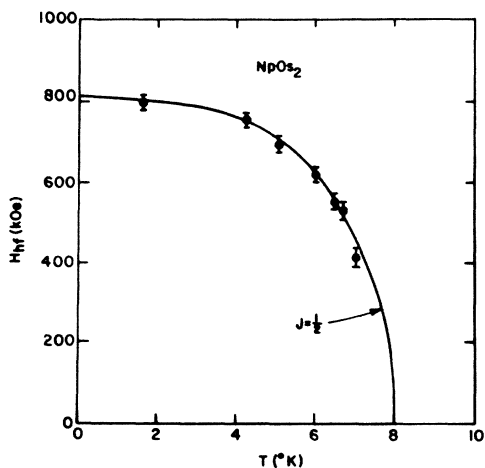


FIG. 9. Temperature dependence of the hyperfine field for NpOs_2 . The solid line represents a $J = \frac{1}{2}$ Brillouin function.

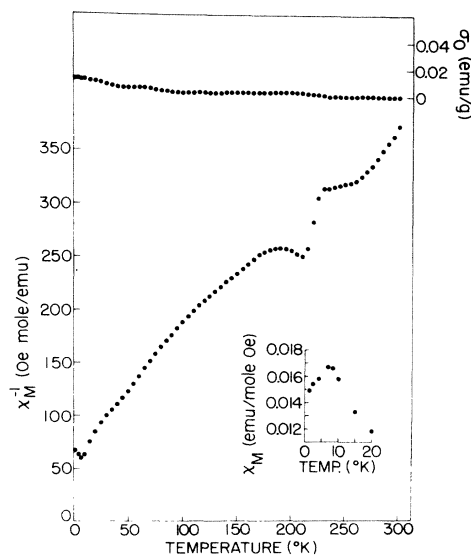


FIG. 10. Temperature dependence of the reciprocal molar susceptibility and σ_0 (see text) for NpIr_2 . The inset shows an enlarged plot of the susceptibility maximum near 7.5°K.

to 1.5°K to define the peak more clearly. The presence of magnetic ordering is substantiated by the NGR spectrum at 4.2°K; the hyperfine field has been determined only at this temperature and has a value of 1080 kOe. More detailed data as a function of temperature have been obtained by Gal *et al.*,¹⁹ and the saturation hyperfine field of 1220 kOe gives a neptunium moment [via Eq. (3)] of $\sim 0.6\mu_B$.

The susceptibility discontinuity near 220°K together with the complicated temperature dependence above and below this temperature region are presumably associated with some type of change in crystal structure. A similar, but smaller, anomaly is seen in NpRu_2 , and this is associated with a lattice distortion observed by low-temperature x-ray measurements. It is tempting, therefore, to associate the discontinuity in the susceptibility of NpIr_2 with a lattice distortion. We hope to clarify this situation with low-temperature x-ray measurements.

D. NpRu_2

The magnetization curves of NpRu_2 are linear from 3.5 to 13.5 kOe over the entire temperature range. The low-field data fall systematically below the line, and this is consistent with a rather large value of σ_0 (~ 0.05 emu/g) that shows essentially no temperature dependence. This is evident in Fig. 11, which also shows the reciprocal molar susceptibility as a function of temperature. The main feature of this curve is the anomaly around 160°K alluded to above. Resistivity measurements on this compound¹⁸ also show a small reproducible

TABLE I. Magnetic properties of neptunium Laves-phase compounds.

Compound	a_0 (Å)	d_{Np} (Å)	Magnetism ^a	Ordering temp. (°K)	H_{hf}^b (kOe)	Isomer shift ^{b,c} (mm/sec)	μ_{sat}^d
NpAl ₂	7.785	3.371	F	56.5 ± 1	2900 ± 50	0	1.5 ± 0.2
NpOs ₂	7.528	3.258	F	7.5 ± 0.5	760 ± 50	-15 ± 1	0.4 ± 0.1
NpIr ₂	7.509	3.251	AF	7.5 ± 0.5	1080 ± 50	-11 ± 1	0.6 ± 0.1
NpRu ₂	7.446	3.230	P	•••	e	-17 ± 1	•••

^aF, ferromagnetism, AF; antiferromagnetism; and P, paramagnetism.

^bAt 4.2°K.

^cIsomer shifts relative to NpAl₂. Ionic Np³⁺ is approximately +35 mm/sec, and ionic Np⁴⁺ is approximately -10 mm/sec.

^dSaturation moment calculated from Eq. (3).

^eBroadened line indicates unresolved hyperfine splittings.

discontinuity at 163°K. Low-temperature x-ray measurements²⁰ have shown that a tetragonal distortion of the cubic C-15 structure occurs at this temperature. Apart from the anomaly, the susceptibility of NpRu₂ varies quite smoothly with temperature. The susceptibility increases more rapidly with a decrease in temperature below 30°K but is still relatively small (compared with the other Np Laves phases) at 4°K; no evidence of any magnetic ordering down to 1.8°K exists. The absence of magnetic ordering is confirmed by the NGR spectrum at 4.2°K (Fig. 5); the broadness of the single line is most probably related to the known crystallographic distortion. NGR measurements have also been taken in an external field of 44 kOe. The data are difficult to analyze because of uncertainties in the zero-field spectrum, but the results are consistent with *no* local moment. This conclusion is supported by the resistivity measurements of this compound.¹⁸

IV. DISCUSSION

The systematic variation of magnetic properties with neptunium-neptunium distance d_{Np} in the compounds we have studied is demonstrated in Table I. The compound with the largest value of d_{Np} (NpAl₂) has by far the highest transition temperature (56.5°K) and substantially the highest ordered moment ($\sim 1.5\mu_B$). The value of T_c obtained in this study is in agreement with previously published values.^{19,21} Although the high-temperature susceptibility of NpAl₂ does not follow the Curie-Weiss law precisely (Fig. 3), the χ_M^{-1} vs T plot is less curved than for the other compounds. The deviations from linearity may well be associated with crystal-field effects as in the case of NpAl₃¹⁰ (cubic AuCu₃-type structure). The value of the ordered moment, the almost Curie-Weiss behavior, and the linearity of the Arrott plots for NpAl₂ (Fig. 2) all suggest that this is a local-moment system. However, the more fundamental question of whether the 5f electrons are truly localized cannot be answered within the context of the present results.

In the case of NpOs₂, the fractional value of the neptunium moment ($\sim 0.4\mu_B$), the low ordering temperature (7.5°K), the substantial curvature of the χ^{-1} vs T plot (Fig. 7), and the curvature of the Arrott plots near the Curie temperature (Fig. 6) all suggest that the neptunium moment is much less localized than in NpAl₂. Stronger evidence comes from the field dependence of the magnetization at the lowest temperatures. As we noted in Sec. III, an approximate extrapolation of this field dependence to saturation gave a moment ($\sim 0.7\mu_B$ /mole) considerably larger than the moment deduced from the NGR hyperfine field data. It is tempting to suppose, therefore, that the field dependence of the magnetization at the lowest temperatures may be due, in part, to a field-induced band magnetism. If this is true, the field dependence at high fields should be linear, yielding a band susceptibility, and should extrapolate back to zero field to give a

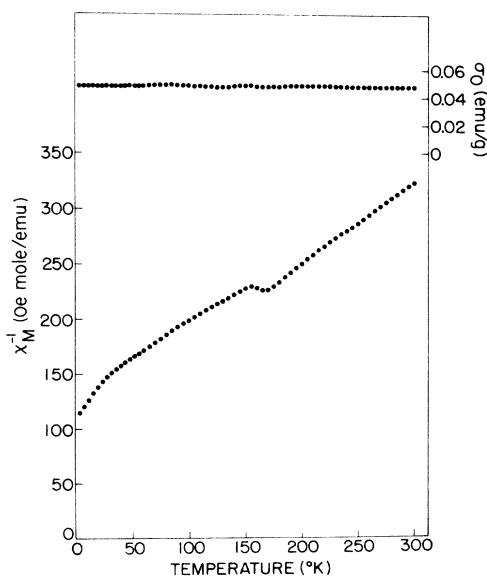


FIG. 11. Temperature dependence of the reciprocal molar susceptibility and σ_0 (see text) for NpRu₂.

value of the spontaneous moment. The four highest field points at 4 °K (Fig. 8) do lie on a good straight line, which yields a susceptibility of 2.5×10^{-2} emu/mole Oe and extrapolates to zero field to give a spontaneous moment ($0.4 \mu_B$ /mole) in agreement with the neptunium moment deduced from NGR results. The magnetic properties of an itinerant ferromagnet have often been discussed. According to Murata and Doniach,²² a relationship exists between the Curie-Weiss constant C determined immediately above the transition temperature and the bulk susceptibility χ at $T=0$ of an itinerant ferromagnet such that

$$2\chi T_c/C = R, \quad (4)$$

where R is a parameter less than unity. Murata and Doniach calculate a value of $R=0.62$ for Sc_3In ($T_c=6^\circ\text{K}$) from experimental data. A similar calculation for NpOs_2 based on the susceptibility value given above, a Curie temperature of 7.5°K , and a value of $C=0.6$ determined from the data in Fig. 7 between 10 and 40°K , also yields $R=0.62$.

The temperature dependence of the susceptibility in both NpIr_2 (Fig. 10) and NpRu_2 (Fig. 11), although obscured by the effects of lattice distortion, appears to be more curved than in the case of NpAl_2 . The small value of the ordered moment in NpIr_2 ($\sim 0.6 \mu_B/\text{Np}$) again suggests that the magnetism is not completely localized. The transition temperature of NpIr_2 , although it orders antiferromagnetically, is essentially identical to that of NpOs_2 , and this correlates with the fact that they have almost the same lattice parameter value (Table I). The value of T_N determined in the present work is slightly larger than that obtained by Gal *et al.*¹⁹ Long-range magnetic ordering does not occur in NpRu_2 , which has the smallest d_{Np} value of the compounds studied here. The NGR data in an external magnetic field suggest that no local moment is present. Presumably, the overlap of the $5f$ electron wave functions in NpRu_2 is sufficient to produce a bandwidth too broad to support a local moment. The low-temperature resistivity of NpRu_2 ¹⁸ has a T^2 dependence, which is usually as-

sociated with spin-fluctuation effects²³; the resistivity of NpOs_2 is typical of a ferromagnet.

The aim of the previous discussion has been to show the systematic change in the electronic structure that accompanies a decrease in the neptunium-neptunium distance on going from NpAl_2 to NpRu_2 . Thus, NpAl_2 appears to be a good local-moment system with $T_c=56^\circ\text{K}$, and $\mu_{\text{sat}}=1.5 \mu_B$ /mole; NpOs_2 is weakly magnetic (probably itinerant) with $T_c=7.5^\circ\text{K}$, and $\mu_{\text{sat}}=0.4 \mu_B$ /mole; NpIr_2 is weakly magnetic with $T_N=7.5^\circ\text{K}$, and $\mu_{\text{sat}}=0.6 \mu_B$ /mole; and NpRu_2 does not order magnetically but shows evidence, in the resistivity data, of spin-fluctuation effects. We may understand all these results qualitatively in terms of a band model in which the neptunium $5f$ electrons form a narrow band close to the Fermi level. In NpAl_2 , the width Δ of this band is small, and the moment is essentially localized. As d_{Np} decreases, overlap of the $5f$ wave functions and hybridization of the $5f$ states with the spd conduction band causes an increase in Δ and a commensurate delocalization of the $5f$ electrons. This in turn results in a decrease in the amount of unpaired $5f$ spin, which eventually causes the disappearance of local moments. In addition, Δ becomes so large that itinerant magnetism does not occur. Below an Np-Np separation of $\sim 3.23 \text{ \AA}$, magnetic ordering from the neptunium alone is no longer possible. In the NpX_2 Laves phases in which X is a $3d$ element, which will be considered in a separate publication (see also Ref. 19), magnetic ordering again occurs even though d_{Np} is less than in NpRu_2 . This is associated with the magnetic behavior of the $3d$ partner and the possibility of inducing a moment on the neptunium atom as a consequence of the exchange field of the $3d$ atom.

ACKNOWLEDGMENTS

The authors would like to thank A. W. Mitchell and S. D. Smith for experimental assistance. Useful discussions have been held with S. Doniach, F. Y. Fradin, A. J. Freeman, A. R. Harvey, J. Hertz, and D. D. Koelling.

*Work performed under the auspices of the U. S. Atomic Energy Commission.

¹D. J. Lam and A. T. Aldred, in *The Actinides: Electronic Structure and Related Properties*, edited by A. J. Freeman and J. B. Darby, Jr. (Academic, New York, 1974).

²A. J. Freeman and D. D. Koelling, *J. Phys. (Paris)* **33**, C3-57 (1972).

³R. Jullien, E. Galleani d'Agliano, and B. Coqblin, *Phys. Rev. B* **6**, 2139 (1972).

⁴H. Hill, in *Plutonium 1970 and Other Actinides*, edited by W. N. Miner (AIME, New York, 1971).

⁵B. D. Dunlap, G. M. Kalvius, S. L. Ruby, M. B. Brodsky, and D. Cohen, *Phys. Rev.* **171**, 316 (1968).

⁶A. T. Aldred, *J. Appl. Phys.* **37**, 671 (1966).

⁷L. L. Sparks and R. L. Powell, *J. Res. Natl. Bur. Std. (U.S.)* **76A**, 263 (1972).

⁸H. Danan, A. Herr, and A. J. P. Meyer, *J. Appl. Phys.* **39**, 669 (1968).

⁹S. Blow, *J. Phys. C* **3**, 835 (1970); J. Gal, Z. Hadan, E. R. Bauminger, I. Nowik, S. Ofer, and M. Perkal, *Phys. Lett. A* **31**, 511 (1970).

¹⁰A. T. Aldred, B. D. Dunlap, and D. J. Lam, *AIP Conf. Proc.* **18**, 366 (1974).

¹¹A. Arrott, *Phys. Rev.* **108**, 1394 (1957).

¹²See, e. g., W. E. Gardner and T. F. Smith, *Proceedings of the Eleventh International Conference on Low Temperature Physics, St. Andrews, 1968*, edited by

- J. F. Allen, D. M. Finlayson, and D. M. McCall (University of St. Andrews Printing Dept., St. Andrews, Scotland, 1969), Vol. 2, p. 1377; F. A. Wedgwood, *J. Phys. C* 5, 2427 (1972).
- ¹³See, e.g., R. M. Bozorth, in *Ferromagnetism* (Van Nostrand, New York, 1951), pp. 484 *et seq.*
- ¹⁴A. T. Aldred, B. D. Dunlap, A. R. Harvey, D. J. Lam, G. H. Lander, and M. H. Mueller, *Phys. Rev. B* 9, 3766 (1974).
- ¹⁵W. J. Nellis, A. R. Harvey, G. H. Lander, B. D. Dunlap, M. B. Brodsky, M. H. Mueller, J. F. Reddy, and G. R. Davidson, *Phys. Rev. B* 9, 1041 (1974).
- ¹⁶B. D. Dunlap (unpublished).
- ¹⁷G. H. Lander and M. H. Mueller (private communication).
- ¹⁸A. R. Harvey, *Solid State Commun.* (to be published).
- ¹⁹J. Gal, Z. Hadari, U. Atzmony, E. R. Bauminger, I. Nowik, and S. Ofer, *Phys. Rev. B* 8, 1901 (1973).
- ²⁰M. H. Mueller (private communication).
- ²¹B. D. Dunlap, M. B. Brodsky, G. M. Kalvius, G. K. Shenoy, and D. J. Lam, *J. Appl. Phys.* 40, 1495 (1969).
- ²²K. K. Murata and S. Doniach, *Phys. Rev. Lett.* 29, 285 (1972).
- ²³See, e.g., S. Doniach in *AIP Conf. Proc.* 10, 549 (1972).